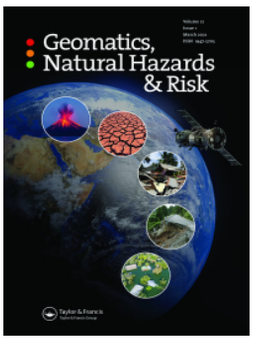

Geomatics, Natural Hazards and Risk

ISSN: (Print) (Online) Journal homepage: https://www.tandfonline.com/loi/tgnh20

Optimal decision making in post-hazard bridge recovery strategies for transportation networks after seismic events

Sungsik Yoon, Wonho Suh & Young-Joo Lee

To cite this article: Sungsik Yoon, Wonho Suh & Young-Joo Lee (2021) Optimal decision making in post-hazard bridge recovery strategies for transportation networks after seismic events, Geomatics, Natural Hazards and Risk, 12:1, 2629-2653, DOI: 10.1080/19475705.2021.1961881

To link to this article: https://doi.org/10.1080/19475705.2021.1961881

Published online: 30 Aug 2021.

GEOMATICS, NATURAL HAZARDS AND RISK
2021, VOL. 12, NO. 1, 2629–2653
https://doi.org/10.1080/19475705.2021.1961881

Taylor & Francis
Taylor & Francis Group

Optimal decision making in post-hazard bridge recovery strategies for transportation networks after seismic events

Sungsik Yoon[a], Wonho Suh[b] and Young-Joo Lee[c]

[a]Department of Civil and Environmental Engineering, University of Illinois at Urbana-Champaign, Urbana, IL, USA; [b]Department of Transportation and Logistics Engineering, Hanyang University, Ansan, Republic of Korea; [c]Department of Urban and Environmental Engineering, Ulsan National Institute of Science and Technology Ulsan, Republic of Korea

ABSTRACT

In this study, optimal post-hazard bridge recovery strategies were proposed for transportation networks under seismic conditions. To predict the performance of the transportation network, a robust performance measure, total system travel time (TSTT), was employed, and an artificial neural network (ANN)-based surrogate model was developed to enable an accelerated Monte Carlo analysis. In addition, a sensitivity analysis based on the benefit–cost ratio was proposed to support optimal decision making immediately after an earthquake. To demonstrate the proposed methodology, an actual transportation network in South Korea was adopted, and a network map was reconstructed based on geographic information system (GIS) data. A surrogate model for network performance evaluation was constructed using training data generated based on historical earthquake epicenters. In addition, the damage ratio and required recovery days according to the damage states of bridges were employed to perform network recovery analysis. For the numerical analysis, a limited budget was set for each scenario, and the recovery and damage curve were compared with existing priority strategy. The numerical results showed that the priority strategy of bridge restoration determined through the benefit–cost analysis generated a faster recovery curve and significantly reduced the damage, as compared to existing strategy. Therefore, it is concluded that the proposed methodology enables optimal decision making and also helps risk management that can minimize the economic damage.

ARTICLE HISTORY
Received 18 March 2021
Accepted 25 July 2021

KEYWORDS
Benefit–cost analysis; optimal restoration strategy; seismic resilience; transportation network; total system travel time; artificial neural network

1. Introduction

Owing to natural disasters and man-made hazards, critical urban infrastructure such as transportation, water, gas, and power networks experience significant direct

CONTACT Young-Joo Lee ylee@unist.ac.kr

damage, and other lifeline structures also experience long-lasting secondary damage. Generally, lifeline infrastructures are densely distributed at the center of a city and consist of systems that are interdependent with other lifeline systems. Therefore, damage to these structures in the event of natural disasters such as earthquakes can lead to cascading failures.

Transportation networks including bridges, are constructed nationwide to support industrial, residential, and economic activities, conveying a wide range of products and supplies between multiple sources and destination nodes. The importance of transportation networks can be recognized even after extreme events occur, because it plays an important role in ensuring access and executing recovery plans for other infrastructure systems, along with providing public support. In particular, the bridge system's ability to reduce and repair damage to the transportation network has been demonstrated in historical earthquakes such as the Loma Prieta (1989), Northridge (1994), and Tohoku (2011) earthquakes. Bridge structures are classified as the most important facilities for minimizing bottlenecks in the event of an earthquake and allowing mutual access for public support. In the case of prolonged damage to bridge structures, significant secondary damage to commercial and industrial activities can occur. In addition, bridge structures are constructed using various design and construction methods depending on the location and environment of geospatially distributed sites. Thus, it is important to establish a recovery strategy of bridge structures considering structural and material characteristics as well as the location and magnitude of the earthquake.

For performance evaluation of transportation networks, various performance measures can be considered depending on the targeted accuracy of analysis and computational cost. If the connectivity between the source and the destination node is crucial, the damage state of bridge can be simply expressed as a bi-state (connect or not). However, if there is change in the bridge demand according to the damage, newer performance measures, such as the maximum flow capacity, should be employed. With the development of various traffic analysis tools in recent years, more practical performance measures have been proposed to predict the travel time of the entire network. Because there are various performance measures depending on the analysis condition or user purpose, the proper measure should be determined.

Various studies on seismic risk assessments have been conducted to evaluate the urban area (Parvez 2013; Liu et al. 2019) and degradation of lifeline infrastructures such as water (Yoon et al. 2020), gas (Yoon et al. 2019), and power (Nuti et al. 2007) networks. With regard to transportation networks, Nuti et al. (2009) proposed a seismic risk assessment method for various utility systems and applied this methodology to an urban-level transportation network. Lee et al. (2011) introduced a non-sampling-based matrix-based system reliability method to evaluate the post-hazard flow capacity of a transportation network. Rokneddin et al. (2013) developed a system reliability assessment method based on finite-state Markov Chain Monte Carlo (MCMC) simulations and performed a seismic risk analysis of highway transportation networks, along with suggesting ranking and priority strategies for retrofitting bridge components. Moreover, Yoon et al. (2020) performed an accelerated seismic risk assessment of a transportation network composed of bridges based on an ANN model

to decrease the computational time required for the reliability analysis of a high-dimensional system. However, these studies evaluated the network performance without considering seismic resilience, including changes in network performance owing to recovery over time.

In recent years, research has been actively conducted to quantify the resilience of lifeline systems following the restoration of facilities. Traditionally, resilience can be represented by a recovery curve that reflects various factors such as flexibility, robustness, recovery, and rapidity of the network system (Mebarki et al. 2016; Loperte et al. 2019). For resilience estimation, Ayyub (2014) proposed the definition, metrics, and valuation of systems resilience considering multi-hazard environments, and Achillopoulou et al. (2020) provided a resilience roadmap for monitoring of transport infrastructure exposed to multiple hazards. In addition, several recent studies have measured the resilience of various lifeline systems such as gas and power networks (Ouyang and Wang 2015), water and power networks (Sharma and Gardoni 2020), hospitals (Cimellaro et al. 2010), buildings (Masoomi et al. 2020), and seaports (Shafieezadeh and Burden 2014). For transportation networks, Argyroudis et al. (2021) proposed a resilience assessment framework including physical vulnerability, recovery and total losses, and they applied the proposed framework in bridge under seismic condition. Mitoulis et al. (2021) provided restoration models for quantifying flood resilience of bridges, and Misra et al. (2020) presented post-hazard restoration of roadways and bridges based on the empirical data and expert opinion. In addition, Farzam et al. (2018) evaluated the rapid bridge performance methodology against seismically induced landslides. Based on the resilience analysis of individual network components, numerous researchers extended resilience assessment to network analysis for decision making. For this purpose, Bocchini and Frangopol (2012) conducted optimal restoration plans for bridges of a transportation network by using a genetic algorithm. However, their study only provided a set of Pareto solutions for the recovery strategy. Alipour and Shafei (2016) proposed a traffic allocation model based on the condition of the origin–destination (O–D) pairs, taking into account the aging effect of network components; their model evaluated the direct loss, indirect loss, and resilience curves in the California transportation network. Zhang et al. (2017) presented a risk mitigation methodology for road-bridge networks based on resilience and conducted research on the change in the resilience curve according to the adopted post-hazard recovery strategy. Decò et al. (2013) conducted research on probabilistic recovery patterns and recovery strategies based on a decision tree analysis and compared the resilience measures, direct costs, and recovery times according to various strategies. In addition, Islam et al. (2021) proposed an index-based social resilience measure to conduct spatio-temporal assessment against the tropical cyclones in coastal Bangladesh.

Previous studies have adopted relatively simple measures such as connectivity analysis (Poljanšek et al. 2012; Yoon et al. 2018) or maximum flow capacity (Lee et al. 2011; Tak et al. 2019) and have not introduced robust performance measures such as total system travel time (TSTT), which can accurately represent the performance of transportation networks. In addition, the previously proposed methodologies have only been applied to relatively simple and low-dimensional network (Sanchez-Silva

et al. 2005; Nuti et al. 2009). Moreover, in previous studies, restoration priorities were proposed by simply clustering the network with a number of bridges or by employing region-based strategies for measuring resilience. However, for optimal post-hazard recovery strategies, it is necessary to provide a priority strategy taking into consideration the construction cost and repair cost of the bridge, the indirect damage cost due to network performance degradation, and the calculation of the resilience curve. In this study, the seismic resilience is defined as the intrinsic system ability to overcome the disturbance and recover to a complete system functionality after seismic conditions.

Therefore, this study proposes an optimal post-hazard bridge recovery strategy for a system-level transportation network considering the performance measure TSTT. To reduce the significant computational time required for TSTT calculation, an artificial neural network (ANN)-based surrogate model was adopted. The surrogate model allows the accelerated seismic resilience curve to be evaluated even in a high-dimensional transportation network with reduced time cost. In particular, a restoration priority strategy was proposed based on a benefit–cost analysis, and the resilience curve and damage cost were calculated according to the limited repair cost of three different scenarios. The demonstrated example shows that the proposed methodology enables better decision-making, as compared to previous strategies, by providing optimal recovery scenarios with limited financial resources and helps minimize the direct and indirect damage.

2. Theoretical background

2.1. Seismic attenuation law

An earthquake is a phenomenon in which the energy stored in the mantle is transferred to the exterior surface, causing the ground surface to shake during the rupture of the fault. Various types of ground motion can be generated depending on geotechnical environments and the seismic attenuation path through which energy is transferred to the surface. To simplify the expression of this complex phenomenon of radiated energy, the ground motion prediction equation (GMPE) is mainly utilized (Boore et al. 2003). Traditionally, the GMPE is calculated as a mean intensity measure according to the earthquake magnitude, distance from the source to site, vibration period, and site class (Joyner and Boore 1993). In this study, the GMPE proposed by Emolo et al. (2015) was utilized, which is expressed by 222 datasets measured at 132 stations in South Korea through a nonlinear regression analysis. In their research, five coefficients of GMPE were determined as −5.15, 0.95, −0.92, −0.0003, and 0.208, respectively, in South Korea.

In addition, inter-event and intra-event terms were adopted to represent the uncertainty of ground motion (Wagener et al. 2016). The inter-event term represents the uncertainty of the seismic wave characteristics such as earthquake magnitude or vibration period, while the intra-event term represents the amplified or attenuated ground motion according to the attenuation path or condition. The standard deviation of inter- and intra-events are assumed to be 0.14 and 0.29, respectively (Tak

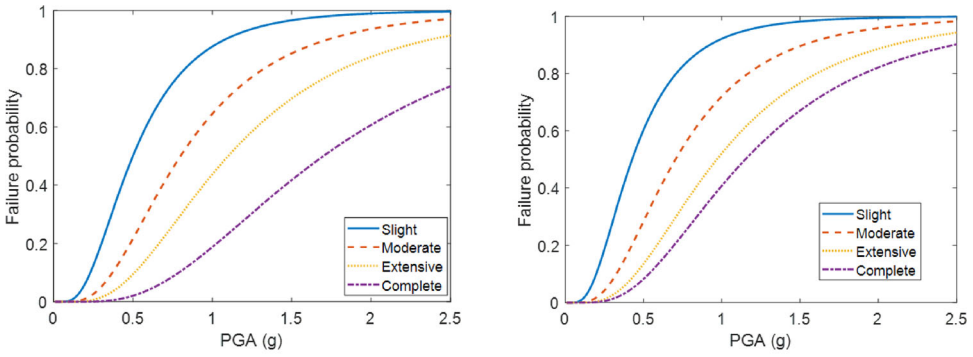

Figure 1. Seismic fragility curves of RC slab and PSC I bridge structures.

et al. 2019), and the spatially correlated equation proposed by Goda and Hong (2008) was used. More detailed description can be found in literature (Yoon et al. 2020).

2.2. Seismic vulnerability analysis of bridge structure

Once ground motion at the location of bridges is generated, the failure probability of the bridge structure can be calculated. The US Federal Emergency Management Agency (FEMA) classifies the damage function according to the geographical location, spectral accelerations (SA), and structural characteristics of the structure such as seismic design, number of spans, structure type, pier type, abutment, bearing type, and span continuity (FEMA 2003). According to HAZUS-MH, it was reported that the SA accurately predicts the failure probability of the bridge structure among other intensity measures, and the failure probability is represented by two parameters (mean and standard deviation) of the lognormal curve based on empirical earthquake data. In addition, the damage states are divided into five levels depending on the degree of damage or the rapid repair time of the structural component. Figures 1a, b shows the seismic fragility curve in case of RC slab and PSC I bridge structures.

To estimate repair costs, it is necessary to evaluate the appropriate damage ratio based on the damage states. In HAZUS-MH, the damage ratio of the bridge structure is evaluated as the ratio of repair cost to construction cost according to the damage state of the bridge. Table 1 presents the range of damage ratio, adopted damage ratio, and mean recovery days according to the damage states of the bridge structure. In this study, the damage ratio for each damage state was allocated as the maximum value of the proposed range of damage ratio, and the required repair cost for each damage state can be expressed as the product of the bridge construction price and the damage ratio (FEMA 2003). Moreover, to present the recovery curve of the transportation network, the recovery days for each bridge structures must be defined. Several researchers have utilized historical data and numerical modeling to demonstrate the restoration capabilities of bridges based on survey-based models (Porter 2004; Padgett and DesRoches 2007) and mathematical expressions (Shinozuka et al. 2003; Bocchini et al. 2012). However, previous models cannot provide sufficient data and consider various bridge materials, types, and designs. Thus, in this study, the

Table 1. Damage ratio and recovery days (FEMA 2003).

Damage state	Range of damage ratios	Adopted damage ratio	Required recovery days
None (DS1)	0	0	0
Slight (DS2)	0.01–0.03	0.03	0.6
Moderate (DS3)	0.02–0.15	0.15	2.5
Extensive (DS4)	0.10–0.40	0.4	75
Complete (DS5)	0.30–1.00	1.00	230

continuous restoration function proposed by the Applied Technology Council (ATC) was adopted based on the empirical data to consider the survey-based system damage state (ATC 1985). As this study focuses on a comprehensive methodology, if realistic restoration and fragility models are considered, the present study can help efficiently decide on restoration strategies.

2.3. Network performance evaluation

TSTT represents the travel time required for moving between entire nodes based on traffic analysis; therefore, it can accurately indicate the degradation of the entire network when external disturbances such as earthquakes occur. To perform traffic analysis, the Emme4 software was adopted, which is an analysis package that optimizes the TSTT to ensure that the traffic flow of the entire network is optimally assigned at the macro level (Florian 2014). The Emme4 software calculates the travel demand through a traffic analysis following four-step travel demand modeling (trip generation, trip distribution, mode choice, and network assignment) taking into account the travel demand and availability of bridge structures within the target network (Sharma S and Mathew 2011). This calculation process enables a variety of transportation plans, such as travel demand forecasting, transportation planning, economic and environmental analysis, and pedestrian and bicycle transportation prediction.

For traffic analysis, basic information regarding the target network and detailed information about the bridge components are required, such as the topology and connectivity of the network, bridge type, types of vehicles, number of lanes, and traffic speed of vehicles. TSTT of the entire network can be obtained by adding all the travel times from source to sink node calculated through the traffic analysis. TSTT is defined as follows:

$$TSTT = \sum_{i=1}^{n_t} AV_i RT_i \tag{1}$$

where AV_i represents the available traffic volume of the i-th link, RT_i represents the time required to travel the i-th link, and n_t represents the number of links in the entire network system. If the traffic capacity of the bridge decreases due to an earthquake, the RT_i will increase which will increase the TSTT, and the change in network performance can be predicted by comparing the TSTT before and after the earthquake.

The RT_i value from the source node to the sink node is the result of the traffic analysis determined according to the bridge condition. If the damage to the bridge

Table 2. Reduced traffic capacity according to the damage state (Murachi et al. 2003; Mackie and Stojadinović 2006).

Damage state	Reduced traffic capacity
None (DS1)	0%
Slight (DS2)	25%
Moderate (DS3)	50%
Extensive (DS4)	75%
Complete (DS5)	100%

becomes severe, the required travel time from node to node tends to increase. For this reason, the modified traffic volume for each damage condition was assumed to consider the reduction in bridge traffic. In this study, five damage states were assumed, and the corresponding reduced traffic capacity was considered based on the previous studies (Murachi et al. 2003; Mackie and Stojadinović 2006). To reduce the flow capacity of damaged bridges, the quarter-based maximum flow capacities are adopted, which are 0%–100% of the original flow capacities with respect to the damage states. Table 2 lists the reduced traffic capacity for each bridge depending on the damage states.

By adopting the TSTT performance measure, in this study, an ANN-based surrogate model was employed to avoid direct traffic analysis. The surrogate model is a pre-trained outcome model that predicts the targeted outcome without direct calculation. It is relatively easy to use, and several researchers have adopted the surrogate model in various research fields. The iterative performance measurement of transportation network was evaluated through the surrogate model. Because the surrogate model utilizes a trained model to enable fast calculations, the ANN-surrogate model is useful in research areas that require excessive iterative calculations such as seismic risk analyses, optimization problems. Although it involves an initial computation cost to generate the training model, once the model is constructed, it has the advantage of being able to use an identical system without additional traffic analysis.

3. Proposed method

3.1. Sensitivity analysis for restoration priority

In the event of external disturbances in transportation network, rapid and accurate recovery plans must be established to rationalize the distribution of repair costs. If the local government has sufficient funds, an ideal restoration plan would be to repair all bridges simultaneously. However, the funds that can be used for bridge repair are limited and depend on the timing and condition of the damaged structure and the financial support. Therefore, it is important to plan the restoration strategy, starting with high-priority bridges considering limited repair costs. To confirm the sensitivity of a bridge structure, Lee et al. (2011) and Tak et al. (2019) proposed importance measures such as the reduction factor of the bridge and the TSTT increment factor (TIF). To determine recovery priority, the proposed equation can be expressed as the sensitivity to the complete collapse of the i-th bridge when an earthquake occurs:

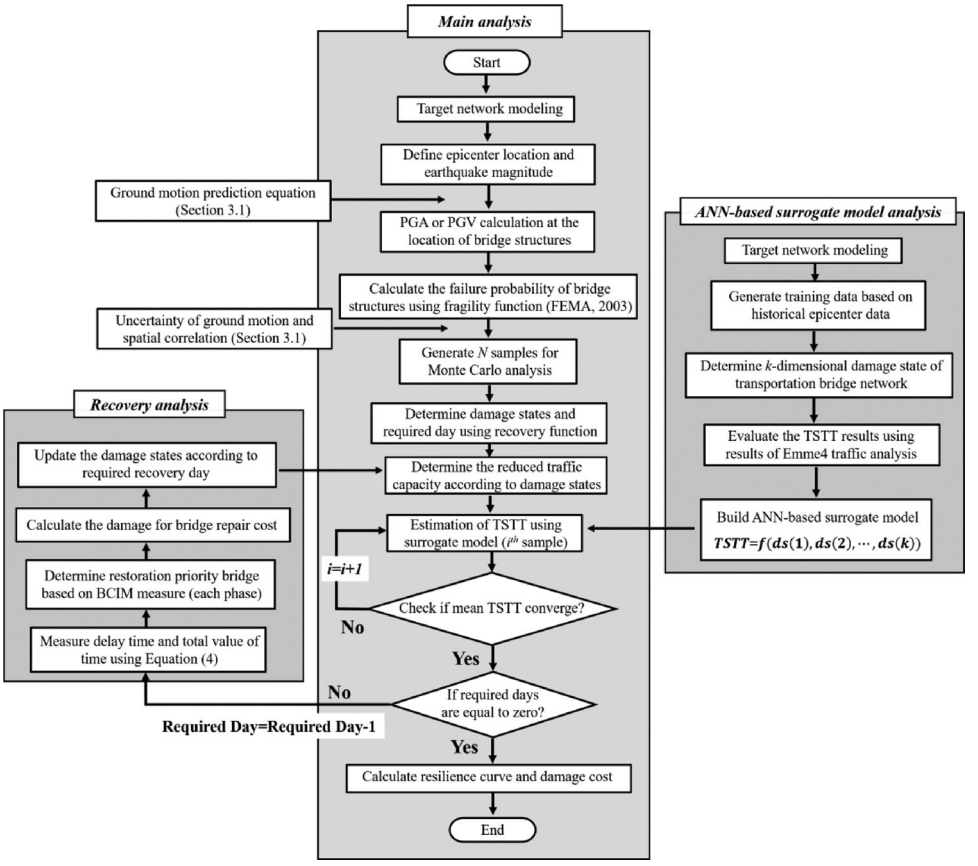

Figure 2. Flow chart of optimal post-hazard recovery strategies.

$$TIF_i = 1 - \frac{TSTT_{\mu_Q|B_i}}{TSTT_{\mu_Q}} \tag{2}$$

where TIF_i indicates the sensitivity value of the i-th bridge, $TSTT_{\mu_Q}$ indicates the mean TSTT (μ_Q) value under seismic conditions, and $TSTT_{\mu_Q|B_i}$ indicates the mean TSTT value when complete collapse of the i-th bridge (B_i) occurs.

However, the previously proposed TIF does not determine the restoration priority reflecting the repair cost of each bridge. Therefore, this study proposes a benefit–cost measure for sensitivity analysis. Because the proposed benefit–cost-based restoration strategy reflects the bridge restoration cost and network performance simultaneously, it is possible to establish an optimal restoration strategy with a limited budget compared to the previous TIF measure. For benefit–cost analysis, a benefit–cost importance measure (BCIM) was defined as the ratio of the decreased indirect damage cost of the network to the repair cost of the i-th bridge:

$$BCIM_i = \frac{IC_i}{DC_i} \tag{3}$$

where $BCIM_i$ represents the benefit–cost analysis-based importance measure of the i-th bridge, DC_i represents the direct damage cost of the i-th bridge, and IC_i represents the decreased indirect damage cost according to the repair of the i-th bridge.

In addition, the value of time (VOT) was adopted to represent the indirect damage as cost, which is defined as the increased daily travel cost for public travel due to construction work. VOT is the cost derived from the driver's time loss due to detouring or rerouting caused by deteriorated road conditions (Daniels et al. 2000). This factor is calculated by taking into account the value of time traveled for the section, vehicle operation cost, and overall accident rates (vehicle-kilometers). Therefore, it can be calculated in different ways depending on the environment and conditions of each country or region, such as prices, average daily traffic, and vehicle type (Choi et al. 2007). For this reason, selecting an appropriate VOT considering the characteristics of the target network can have a significant influence on the results of the analysis. The total VOT with increasing total travel time can be calculated using the following equation:

$$TV_i = DT_i \times VOT \times AADT \tag{4}$$

where TV_i represents the total indirect damage cost incurred in the i-th days, DT_i represents the delay time due to the earthquake, and $AADT$ represents the average annual daily traffic.

3.2. Model construction

A comprehensive seismic resilience estimation model based on a three-step analysis was proposed to perform optimal decision-making in the post-hazard recovery strategy for transportation networks. The proposed model consists of a main analysis phase including target network construction, ground motion prediction, and damage states determination; an ANN-based surrogate model analysis phase for TSTT estimation; and a recovery analysis phase for recovery priority calculation with a benefit–cost analysis based on direct and indirect damage. Figure 2 shows the entire flow chart of the proposed research method.

In previous studies, the mean network performance was calculated using an iterative traffic analysis in the main phase (Kim et al. 2008; Chang 2010). However, to avoid direct TSTT calculation, an ANN-based surrogate model analysis phase was proposed in this study. The network topology and connectivity matrix are required to construct a surrogate model, and basic road network information is required to predict the TSTT based on the traffic analysis. When the target network is reconstructed, it is necessary to determine the location and magnitude of the input earthquake to generate training data. Also, various k-dimensional damage state combinations need to be generated to construct the surrogate model. The input of training data is a k-dimensional damage state vector, and the output data is defined as the TSTT computed through traffic analyses using Emme4; the surrogate model can be constructed using the ANN.

In the main analysis phase, once the target network modeling is reconstructed, the possible location and magnitude of the epicenter must be defined. Using the GMPE,

ground motion at the target network can be generated in terms of peak ground acceleration (PGA) or peak ground velocity (PGV) depending on the epicenter. If the PGA or PGV is calculated at the location of bridge structures, the failure probability of the bridges can be evaluated based on the fragility functions, which are explained in Section 2.2 (FEMA 2003). To guarantee the convergence of the network performance, a sufficient number of sampling needs to be generated. The damage state of the bridge is determined by comparing the failure probability with the inverse transform sampling method between 0 and 1 by considering the uncertainty of ground motion (uncertainty matrix is considered as the standard deviation for sampling). If the damage states of bridge structures are determined, the required recovery days for each bridge need to be designated according to the damage states based on the recovery function (FEMA, 2003). Then, the reduced traffic capacity is determined based on the damage states. TSTT performance of each sampling is calculated through an ANN-based surrogate model, and calculation is repeated until the mean TSTT converges. If all bridges are fully recovered (required day for recovery is equal to zero), TSTT reaches the minimum value, subsequently the seismic resilience curve can be measure. In addition, the total damage cost is calculated, and the entire main analysis phase is completed. However, if the target network has not been completely recovered, it is necessary to proceed to the recovery analysis phase.

The traffic capacity corresponding to damage states is determined based on Tables 1 and 2. Let us assume that a bridge is in a complete damage state (DS5), which means that the reduced traffic capacity is 100% and the required recovery days are 230. If this bridge moves onto recovery analysis, the required recovery days are updated to 229, and the bridge is still in a complete damage state (DS5) with a reduced traffic capacity of 100%. TSTT estimation and recovery analysis are repeatedly performed for this bridge, and when the number of days to recover is 75, the damage state is updated to an extensive damage state (DS4) with 75% reduced traffic capacity. Likewise, TSTT estimation and recovery analysis continue for the bridge until it becomes a non-damage state (DS1).

In the recovery analysis phase, the indirect damage over total time is calculated by using the increased TSTT in the damaged network, as compared with the normal TSTT of the intact network. Thereafter, the restoration priority is determined based on the BCIM measure to implement the optimal post-hazard recovery strategy. When the bridge to be repaired is determined, the repair cost is calculated as direct damage; the required recovery days is updated with one day reduced and the damage states are modified with updated required recovery days (Table 1). The recovery analysis is repeated until the damage states of the entire network is fully recovered, and the entire analysis is completed.

4. Numerical example

4.1. Problem definition

To demonstrate the proposed method, an actual transportation network located in Pohang, Korea was adopted. The target network was reconstructed based on GIS data, and numerical modeling for traffic analysis was performed based on the road

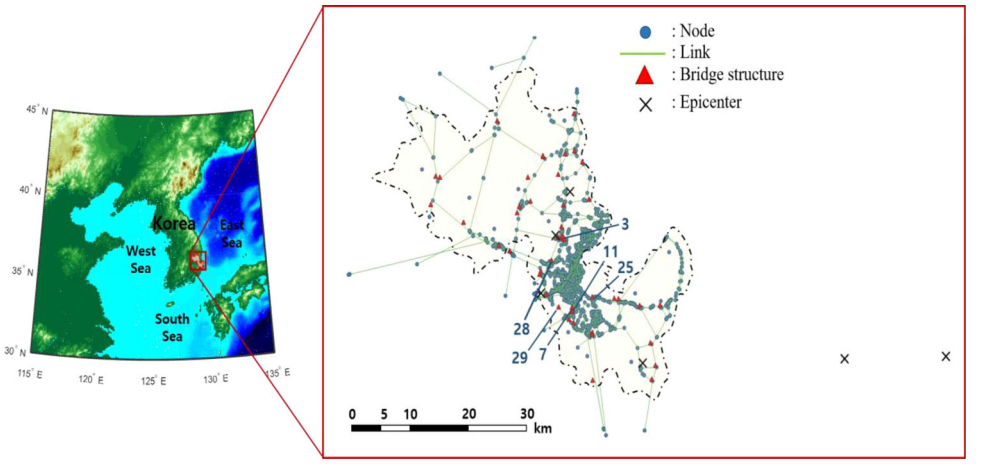

Figure 3. Reconstruction of the target transportation network considering the geographic reference.

and bridge conditions provided by the Korea Infrastructure Safety Corporation. Although it is known that South Korea has a relatively low probability of earthquake occurrence, the Pohang region is located above dense faults of the recent Gyeongju earthquake in 2016 (M 5.8) and Pohang earthquake in 2017 (M 5.4); thus, because of these frequent recent earthquakes, increased attention has been devoted toward seismic risk and seismic resilience estimations.

Figure 3 shows the reconstructed target network, which is composed of 1440 nodes and 3940 links. The nodes are connected through a total of 48 single- or multi-span bridge structures, along highways and local national highways, with an average length of 101.16 m, average bridge width of 17.16 m, average pier height of 5.73 m, average maximum span length of 23.67 m, and average number of spans of 4. For the seismic resilience evaluation, six epicenters were considered based on previous earthquake data provided by the Korea Meteorological Association (KMA).

Figure 4 shows the average daily traffic volume and type of superstructure for the 48 bridges that constitute the target network. Figure 4a shows the average daily capacity of traffic volume for each bridge, and the traffic volume was determined based on statistical data regarding the population and number of households in the Pohang region determined through the 2015 census by Statistics Korea (Korea 2016). Figure 4b shows the five types and ratios of superstructures in the Pohang network.

4.2. Sensitivity analysis for restoration priority

To determine the optimal post-hazard recovery strategies proposed, a sensitivity analysis was performed using Eqs. (2) and (3). The seismic fragility curve provided by Hazus-MH was used; it was classified based on seismic design, number of spans, structure type, pier type, abutment, bearing type, and span continuity (FEMA 2003). In addition, the earthquake occurrence rate in the target network region was assumed to follow the Gutenberg–Richter (G–R) recurrence law to account for the uncertain magnitude of earthquakes occurring in Pohang (Gutenberg and Richter 1944). For

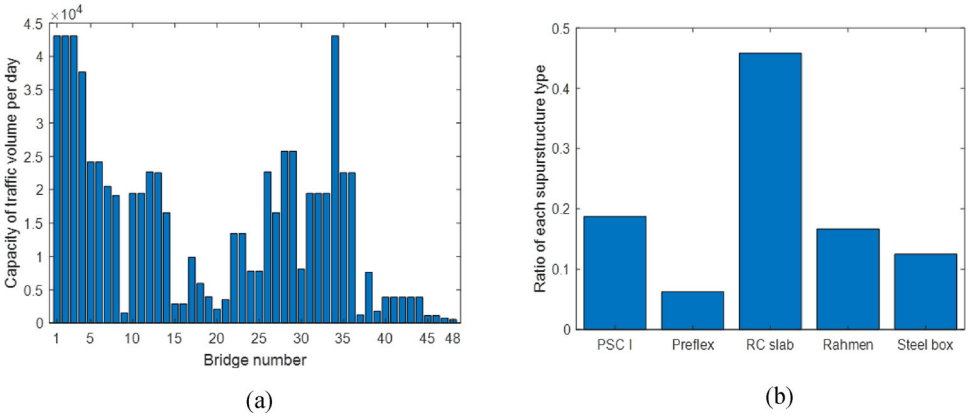

Figure 4. Characteristics of bridge structures in the target network: (a) average traffic volume, and (b) type of superstructure.

the calculation of the occurrence rate in the Pohang area, the historical earthquake data collected by KMA with a magnitude of 3.0 or more from January 1, 1918 to August 22, 2018 were considered, and it was assumed that the location of each epicenter had the same weight. According to previous research results (Tak et al. 2019), the coefficients a and b of the G–R recurrence law were determined to be 2.167 and 0.699, respectively, through regression analyses. The normalized bounded probability density function for earthquake magnitudes between 6.0 and 8.0 is depicted based on the coefficients of the G–R recurrence law (Baker 2013). Figure 5 shows the normalized probability density function for the Pohang area, and the weight of the earthquake magnitude can be considered through the probability density function.

Figure 6 shows the BCIM for each of the 48 bridges considering uncertain earthquake location and magnitude. The importance measure represents the order of the level of improvement in network performance through bridge repairs. In particular, it was confirmed that the priority of bridges according to the BCIM measure is mainly determined by the location of the bridge and the traffic volume (bridge number 28, 3, 25, and 7). As can be observed from the network map in Figure 3, the bridge with highest BCIM was located at the center of the city, and thus, it was found to have a significant impact on the travel time between densely constructed nodes. However, in bridges located around nodes with low traffic volumes or low degrees of freedom around the city center (i.e., a series topology without bypasses or detours), a relatively low BCIM was noted, because these bridges do not significantly affect the access to dense nodes.

Figure 7 shows the importance measure calculated based on the TSTT incremental analysis, which was expressed in Eq. (2). As this is a measure based on network performance excluding the bridge construction cost, the priority of bridge restoration was determined by the location of the bridge or the traffic capacity of the bridge (bridge number 3, 29, 28, 11). Similar to the BCIM results, the priority of bridges located at the center of Pohang was high, which have a significant influence on the traffic volume between clustered nodes. However, the bridges located in the suburbs

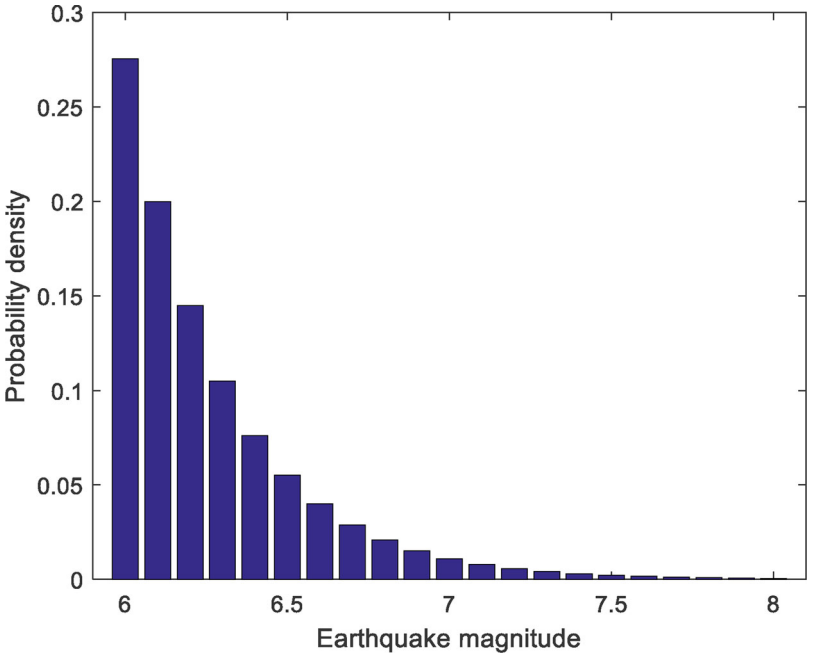

Figure 5. Probability density distribution for uncertain earthquake magnitude.

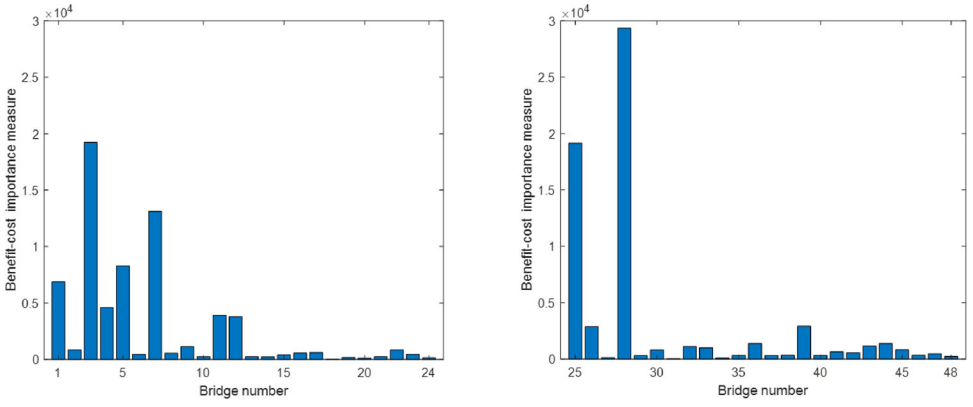

Figure 6. Results of benefit–cost-based importance measure: bridge number (a) 1–24, and (b) 25–48.

of the target network had lower priority because they did not have a significant impact on the network traffic.

Figure 8 represents the bridge construction cost for the Pohang network. Both BCIM and TIF measures prioritize recovery based on the performance of the bridge. However, the BCIM is a measure that reflects the economic budget. Thus, there was a slight difference in the priority indicated by these two importance measures. For example, bridge number 29, with relatively higher construction costs than other bridges, had a lower priority according to the BCIM; however, it had a relatively

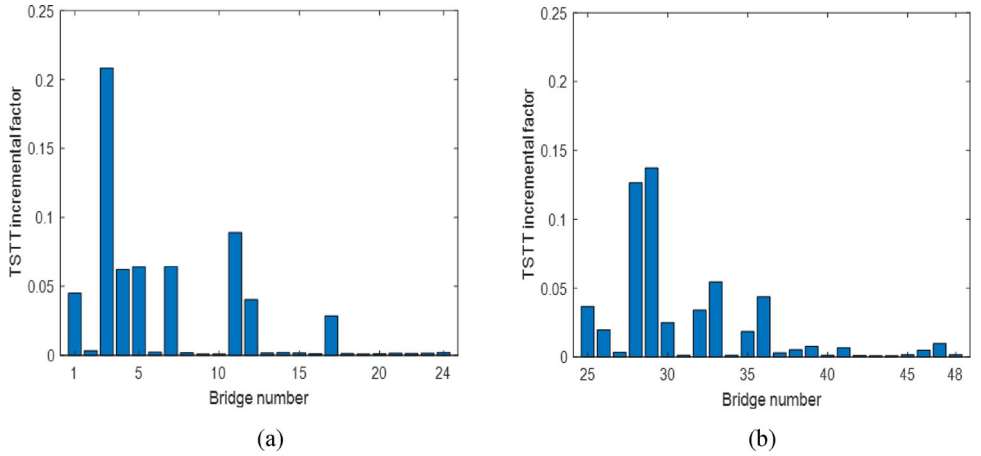

Figure 7. Results of TSTT incremental factor based importance measure: bridge number (a) 1–24, and (b) 25–48.

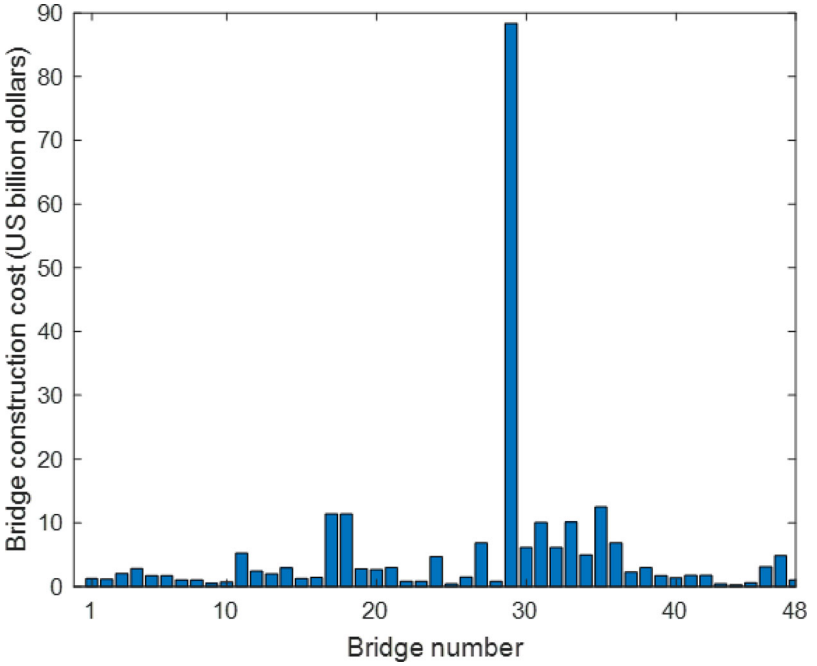

Figure 8. Bridge construction cost for Pohang network.

higher priority according to the TIF because the restoration cost of the bridge was not considered in this priority strategy. In this study, the proposed methodology was verified based on the BCIM by comparing the recovery curve and damage cost according to the priority based on the TIF, and the details are discussed in Section 4.3.

Table 3. Recovery scenarios according to the available budget.

	Phase 1	Phase 2	Phase 3	Phase 4
Scenario A	10%	20%	30%	40%
Scenario B	25%	25%	25%	25%
Scenario C	40%	30%	20%	10%

4.3. Results of optimal post-hazard recovery

In this section, the network recovery curves, direct damage, and indirect damage are compared according to the restoration priority and economic budget based on two measures. For resilience curve, the ANN-based surrogate model trained by Yoon et al. (2020) was employed to predict the TSTT performance of the target network, and 5000 samples were utilized to consider the TSTT convergence. In this study, the benefit–cost ratio-based recovery curve and damage estimation were applied according to the available budget, and the restoration priority based on the TIF was compared to prove the superiority of the proposed method. Table 3 presents the ratio of the available budget for each of the four recovery phases compared to the construction cost of the entire bridge, assuming that the duration of one recovery phase is eight months (see Table 1). Scenario A represents a case where a large budget cannot be used for the cost of repairing a bridge immediately after an earthquake. In the case of Scenario B, the budget can be evenly allocated for all four phases, and finally, Scenario C can support a large budget immediately after the earthquake occurs.

Figure 9 shows the recovery performance of the benefit–cost ratio and TSTT incremental-based recovery strategy according to each available budget scenario when the earthquake magnitude is 6.0, 6.5, and 7.0. TSTT based network performance was normalized by using the minimum and maximum TSTT of target network. Compared to Scenarios A and B, Scenario C tends to recover relatively rapidly because it can repair a large number of bridges immediately after an earthquake using 40% of the recovery cost. Meanwhile, in the case of Scenario A, because only 10% of the total recovery cost can be utilized in phase 1, it can be confirmed that the slope of the performance recovery curve is relatively flat and slow. In addition, even within the same repair budget, the benefit–cost ratio-based recovery strategy shows a more rapid recovery curve compared to the TIF-based recovery strategy, and it can be observed that the time until the network performance cannot be improved (the time when the slope is zero) is shorter. This is because the priorities based on benefit–cost ratios identify bridges that are optimized for performance recovery within a limited budget. In particular, the restoration priority based on the TIF was simply based on performance without considering the repair cost of the bridge, and hence, sufficient bridge repairs could not be made within the budget allocated for each phase. For example, the TIF method was unable to propose an optimal budget allocation as it assigned high priority to bridges such as 29, 33, and 17, which account for a large portion of the overall budget. This phenomenon is clearly observed in Scenario A–C according to the TIF-based results in Figure 9. In particular, in the case of Scenario C, it can be confirmed that the performance recovery proceeds very fast, with an approximate completion time of 50 weeks. Moreover, the initial network performance tended to decrease as

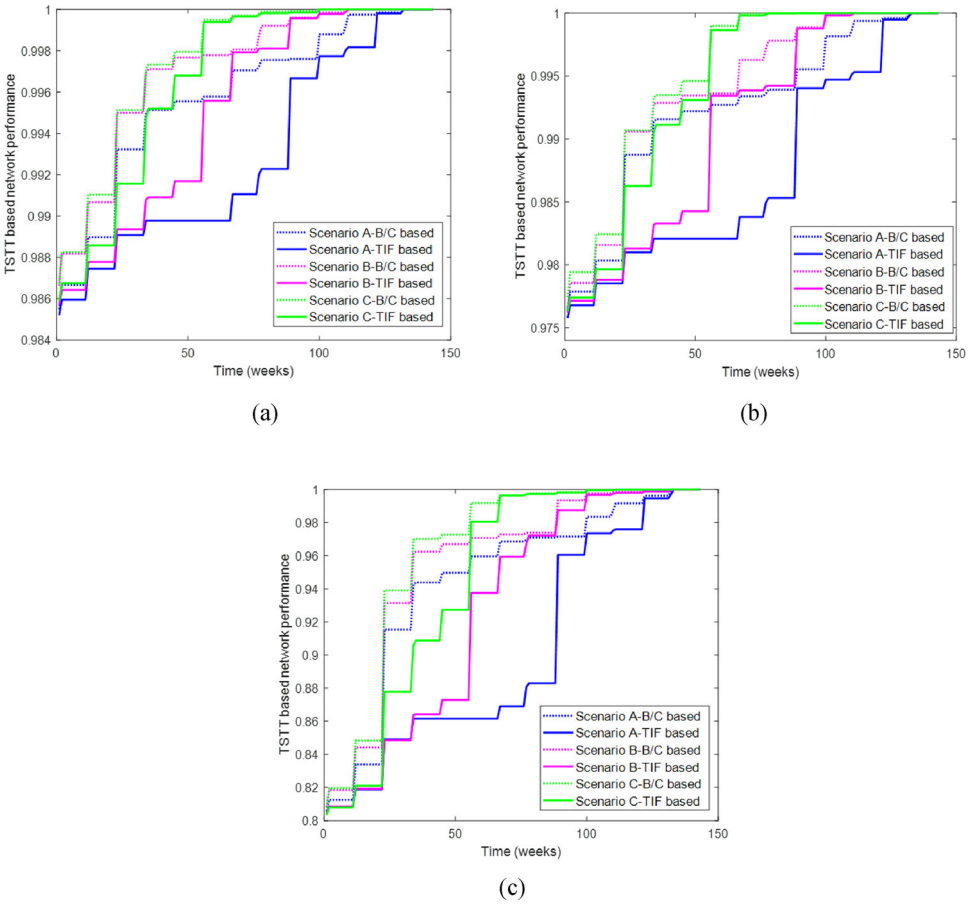

Figure 9. Normalized seismic resilience curve according to recovery strategies based on the benefit–cost ratio and TSTT incremental factor at magnitudes of (a) 6.0, (b) 6.5, and (c) 7.0.

the earthquake magnitude increased, and the slope of the network performance tended to increase as the bridge connected to the center of the target area recovered.

Figure 10 shows the cumulative bridge repair cost according to the network performance recovery. In the case of Scenario C, because the budget immediately after the earthquake is large, it can be confirmed that the slope of the initial direct cost is higher than that in other scenarios. In particular, in TIF-based Scenario C, as bridge number 29 can be repaired, it was confirmed that the direct cost slope of the TIF-based strategy was higher than that of the benefit–cost ratio-based strategy. In TIF-based Scenarios A and B, the increase in direct cost was not significant until week 64 and 32, respectively, because the given budget could not repair bridge 29. However, it can be confirmed that the repair cost until reaching Phase 4 converged regardless of the scenario. This is because the total repair cost is only influenced by the magnitude of the earthquake. In other words, the amount used for repair at each phase may be different, but the total direct damage is the same. Therefore, selecting a bridge with optimal recovery priority for each phase influences the resilience curve of the bridge,

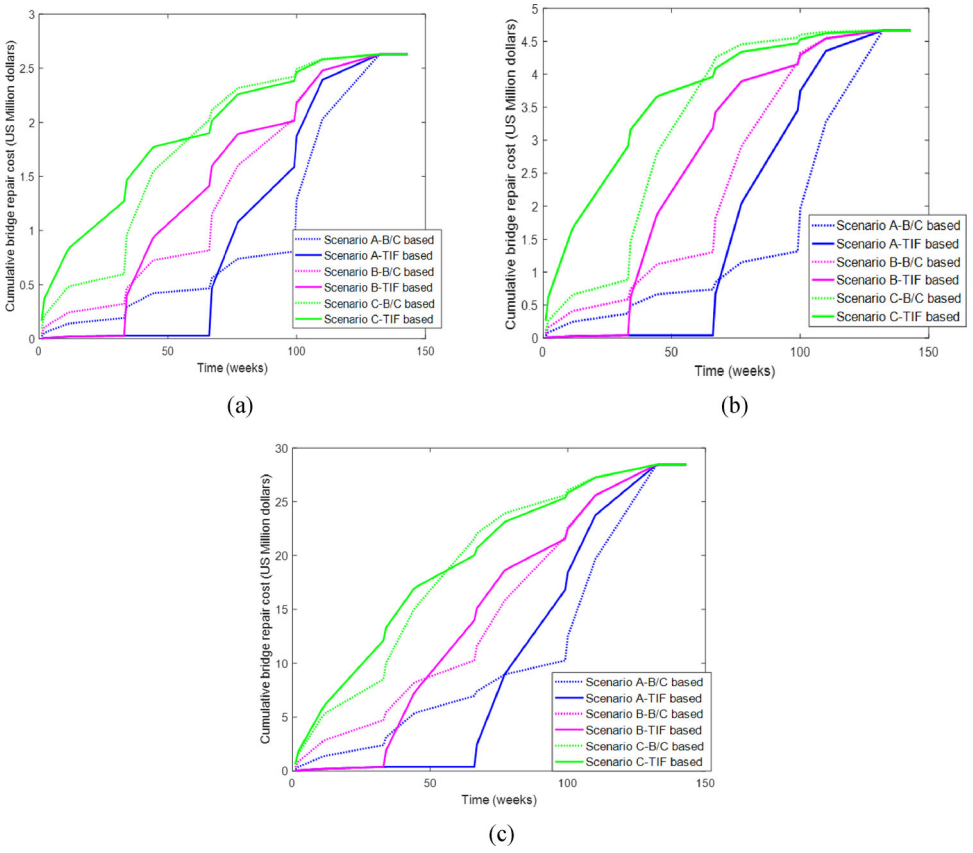

Figure 10. Direct cost estimation according to recovery strategies based on the benefit–cost ratio and TSTT incremental factor at magnitudes of (a) 6.0, (b) 6.5, and (c) 7.0.

which can incur a considerable indirect damage cost and significantly impacts the budget allocation for direct damage cost.

Figure 11 shows the cumulative indirect damage cost according to the performance degradation of the bridge structures. Indirect damage can be defined differently depending on the conditions or categories to be considered. In this study, the total VOT, expressed in Eq. (4), was adopted to express indirect damage as a cost. In particular, it was assumed that the average traffic volume per year was 5,000 vehicles, taking into account the traffic information of Pohang City, and the average VOT (20.63 US dollars per hour) of South Korea that fit the road conditions of the target network was adopted (Choi et al. 2007). As can be observed in Figures 9 and 11, the results of the indirect cost curve show that the benefit–cost ratio-based strategy to recover immediately after an earthquake is lower than that of the TIF-based strategy because the indirect cost of the target network is proportional to the network performance. In addition, in the case of Scenario C, although the allocated budget in Phase 1 was the highest, the indirect cost was significantly lower than that of Scenarios A and B because most of the bridge structures was stabilized more fast. In particular, as the magnitude of the earthquake increases, the network performance decreases rapidly, and the indirect cost tends to increase considerably. Because the

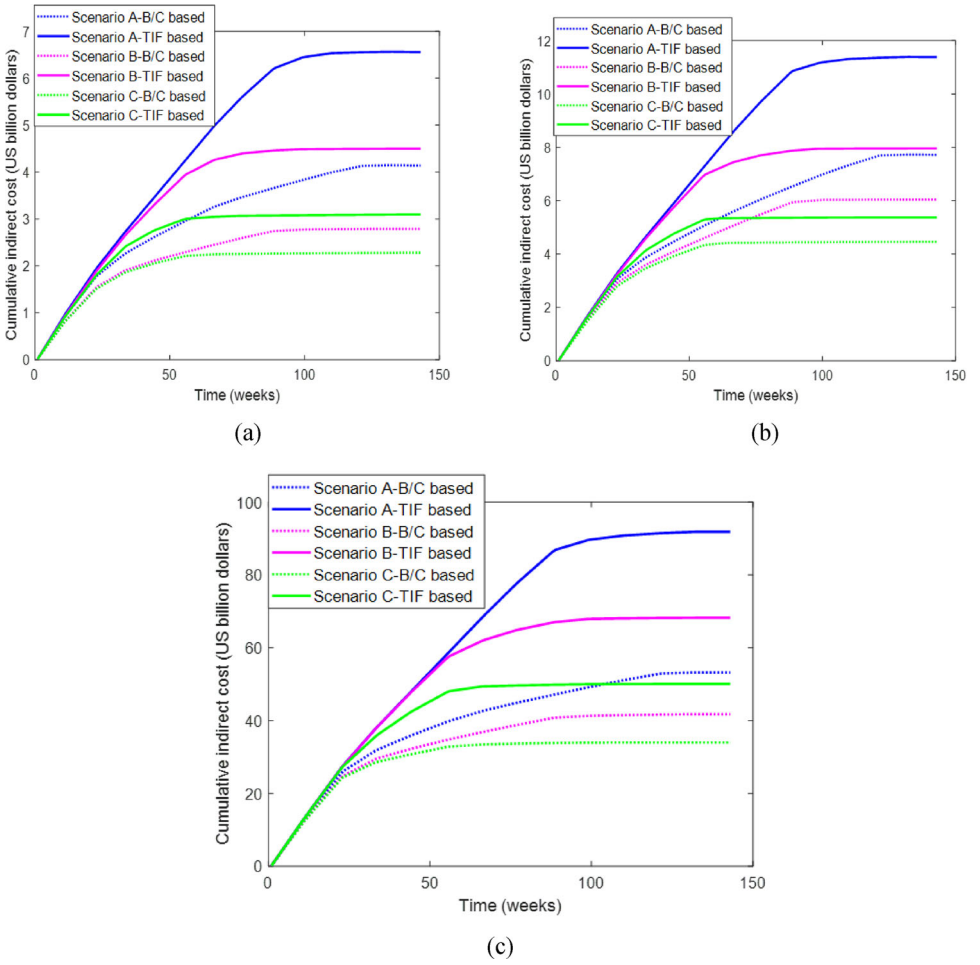

Figure 11. Indirect cost estimation according to recovery strategies based on the benefit–cost ratio and TSTT incremental factor at magnitudes of (a) 6.0, (b) 6.5, and (c) 7.0.

indirect cost can be higher than the bridge repair cost depending on the location and traffic volume of the target network, a recovery plan should be established considering not only the direct cost but also the secondary damage cost.

Figure 12 shows the cumulative distribution of the damage states of bridge structures according to the recovery scenarios of the target network with an earthquake magnitude of 7.0. In each scenario, the benefit–cost-based restoration strategy immediately after the earthquake was more appropriate for the optimal repair of a larger number of bridges within a given budget. Furthermore, as the TIF-based restoration strategy assigns a high priority to bridges with high construction costs, such as bridge number 29, the BCIM–based strategy tends to improve the damage states of the bridges more efficiently in phases 1 and 2. However, because the recovery cost increases as the phase number increases, the bridge ratio of minor damage gradually increases for both strategies. In particular, after 121 weeks of repair (phase 4), it can be confirmed that there is no bridge ratio of the complete damage state in all three scenarios. The numerical results indicate that the epicenter located near the bridge

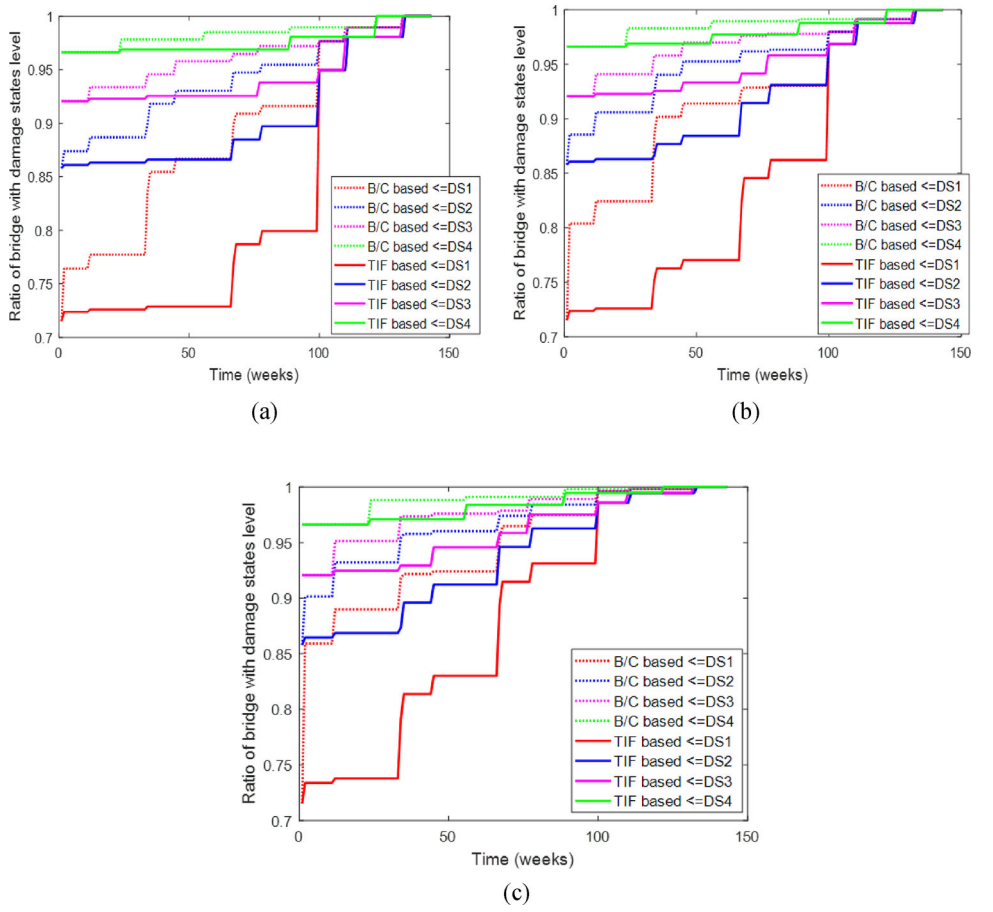

Figure 12. Accumulated ratio of bridges according to the damage state level with an earthquake of M 7.0: (a) Scenario A, (b) Scenario B, (c) Scenario C.

with dense nodes, and the bridge in the complete damage state has a relatively high priority. In addition, it was confirmed that, with a higher budget allocated immediately after the earthquake, the damage rate of the bridge decreased sharply.

Figure 13 shows the spatial distribution of the damage status of bridge structures when the earthquake magnitude is 7.0. Note that the damage becomes more severe as the number increases. Figure 13a shows the spatial distribution of bridges immediately after the earthquake, and Figures 13b, c show the spatial distribution of damaged bridges with BCIM and TIF based on Scenario A after 230 days (phase 1), respectively, and Figures 13d, e show the spatial distribution of damaged bridges with BCIM and TIF based on Scenario A after 460 days (phase 2), respectively. As the bridge structures were recovered, the mean damage level decreased from 0.0888 to a lower damage level. The spatial distribution of damaged bridges shows that the BCIM-based recovery strategy is more efficient than the TIF-based recovery strategy. The BCIM-based scenario shows a lower mean damage level compared with the TIF-based scenario. In particular, the damage level of bridges located in the center of the city was higher because the epicenters were located near the city center. As the

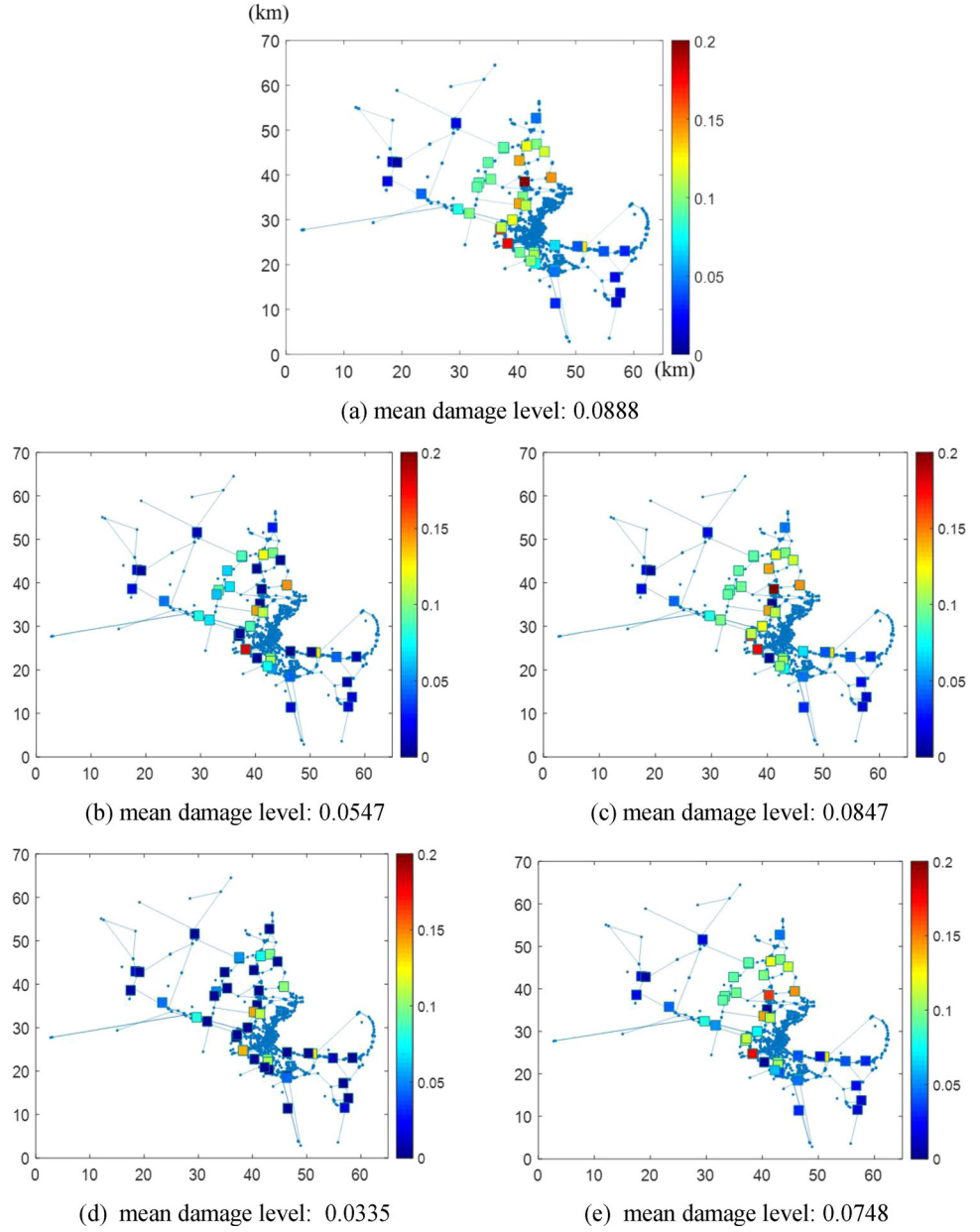

Figure 13. Spatial distribution of damage status of bridge structures (M 7.0) (a) immediately after an earthquake, (b) BCIM based on scenario A after 230 days (c) TIF based on scenario A after 230 days (d) BCIM based on scenario A after 460 days (e) TIF based on scenario A after 460 days (Note that damage is more severe as the number gets bigger).

bridges located near the center recovered (Figure 3), the mean damage level decreased, and the network performance increased.

Figure 14 compares the mean damage level with respect to Scenarios A–C. Figure 14 shows the spatial distribution of the damage status of the bridge structures when the earthquake magnitude is 7.0. Figure 14a shows the spatial distribution of bridges

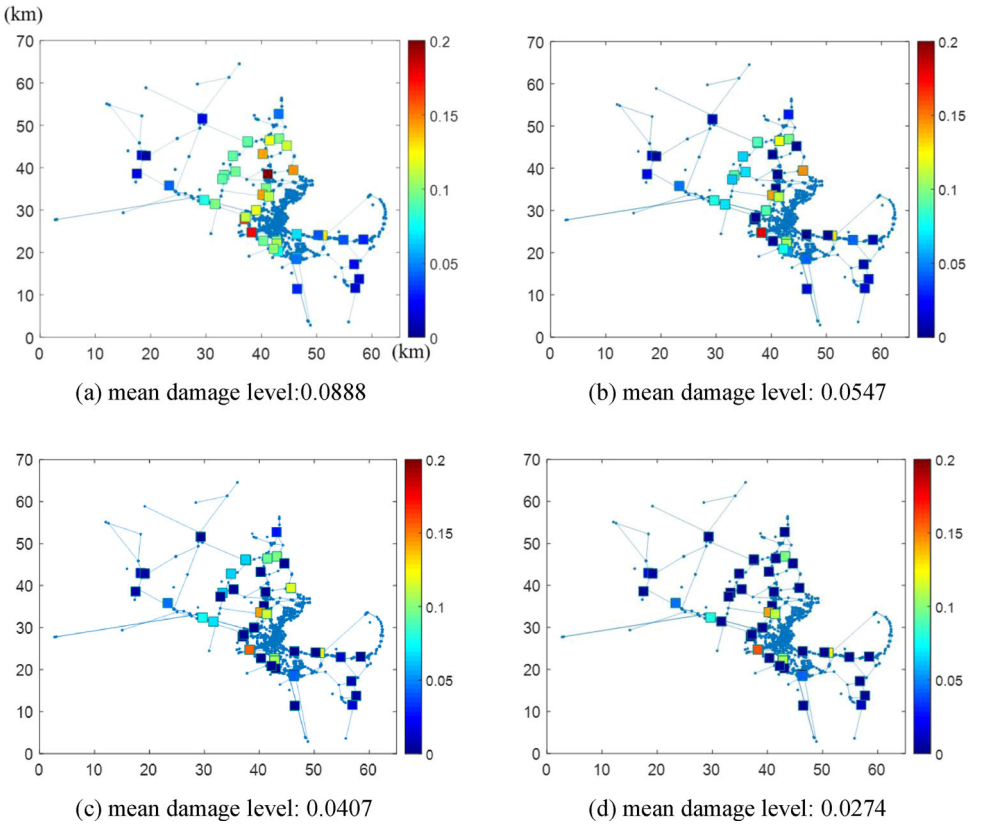

Figure 14. Spatial distribution of damage status of bridge structures (M 7.0) (a) immediately after an earthquake (b) BCIM based on scenario A after 230 days (c) BCIM based on scenario B after 230 days (d) BCIM based on scenario C after 230 days (Note that damage is more severe as the number gets bigger).

immediately after the earthquake, and Figures 14b–d show the spatial distribution of damaged bridges with BCIM for Scenarios A–C after 230 days. Similar to the results of the resilience curve (Figure 9), Scenario C, with a higher budget in Phase 1, represents a lower mean damage level, and the damage level increases as the budget decreases.

5. Conclusion

In this study, the optimal decision-making in post-hazard bridge recovery strategies for transportation networks under seismic conditions was proposed. For accurate performance measurements of the transportation network, a TSTT performance measure based on traffic analysis was adopted, and an ANN-based surrogate model was employed to significantly reduce the computation time of the iterative analysis. In addition, to establish an efficient and economical restoration plan for the transportation network immediately after the earthquake, restoration priorities were presented based on a benefit–cost analysis. In particular, a comprehensive methodology is

proposed, ranging from network recovery curves to direct and indirect damage estimation based on recovery priorities.

To demonstrate the proposed methodology, the present study adopted an actual transportation network consisting of 1440 nodes and 3,490 links with 48 bridge structures. The ANN model used 100,000 data to construct the training equation, and the derived surrogate model was utilized to predict the transportation network TSTT according to the recovery function. For the recovery analysis, a benefit–cost ratio-based sensitivity analysis of the 48 bridges was performed, and the recovery curves and direct and indirect damages according to Scenarios A-C were evaluated. It was found that the proposed method resulted in a faster recovery curve and reduced the indirect damage, compared to the TIF-based recovery priority strategy, which did not account for bridge costs.

The proposed methodology can be utilized for post-hazard decision making in various civil infrastructures. It can be applied not only to transportation networks but also to various interdependent lifeline networks. If more realistic resilience indexes, vulnerability models, and restoration models become available in future studies, the present study can help realistic policy making or budget allocation for efficient recovery strategy and provide a better understanding about transportation networks subject to multiple hazard environments.

Disclosure statement

No Potential Conflict Of Interest Was Reported By The Authors.

Funding

This research was supported by a grant (21SCIP-B146959-04) from Construction technology research program funded by Ministry of Land, Infrastructure and Transport of Korean government. This work was also supported by the 2021 Research Fund (1.210045.01) of UNIST (Ulsan National Institute of Science and Technology).

Data availability

The data are available from the authors upon request.

References

Achillopoulou DV, Mitoulis SA, Argyroudis SA, Wang Y. 2020. Monitoring of transport infrastructure exposed to multiple hazards: A roadmap for building resilience. Sci Total Environ. 746(1):141001.

Alipour A, Shafei B. 2016. Seismic resilience of transportation networks with deteriorating components. J Struct Eng. 142(8):C4015015.

Argyroudis SA, Nasiopoulos G, Mantadakis N, Mitoulis SA. 2021. Cost-based resilience assessment of bridges subjected to earthquakes. IJDRBE. 12(2):209–222.

ATC. 1985. Earthquake damage evaluation data for California. Redwood City, CA.: Technical Rep. ATC-13, Applied Technology Council.

Ayyub BM. 2014. Systems resilience for multihazard environments: definition, metrics, and valuation for decision making. Risk Anal. 34(2):340–355.

Baker JW. 2013. An introduction to probabilistic seismic hazard analysis. White Paper Version 2.1

Bocchini P, Decò A, Frangopol D. 2012. Probabilistic functionality recovery model for resilience analysis. Bridge maintenance, safety, management, resilience sustainability. Boca Raton (FL): CRC Press.

Bocchini P, Frangopol D. 2012. Restoration of bridge networks after an earthquake: Multicriteria intervention optimization. Earthq Spectra. 28(2):427–455.

Boore DM, Gibbs JF, Joyner WB, Tinsley JC, Ponti DJ. 2003. Estimated ground motion from the 1994 Northridge, California, earthquake at the site of the Interstate 10 and La Cienega Boulevard bridge collapse, West Los Angeles, California. Bull Seismol Soc Am. 93(6): 2737–2751.

Chang L. 2010. Transportation system modeling and applications in earthquake engineering. Urbana (IL): Mid-America Earthquake (MAE) Center.

Choi C-H, Park D, Najafi FT, Kim J-L. 2007. Time value of goods movement for project appraisal in South Korea. Transp Res Rec. 1996(1):92–99.

Cimellaro GP, Reinhorn AM, Bruneau M. 2010. Seismic resilience of a hospital system. Structure Infrastructure Engineering. 6(1-2):127–144.

Daniels G, Stockton WR, Hundley R. 2000. Estimating road user costs associated with highway construction projects: simplified method. Transp Res Rec. 1732(1):70–79.

Decò A, Bocchini P, Frangopol DM. 2013. A probabilistic approach for the prediction of seismic resilience of bridges. Earthq Eng Struct Dyn. 42(10):1469–1487.

Emolo A, Sharma N, Festa G, Zollo A, Convertito V, Park JH, Chi HC, Lim IS. 2015. Ground-motion prediction equations for South Korea Peninsula. Bull Seismol Soc Am. 105(5):2625–2640.

Farzam A, Nollet MJ, Khaled A. 2018. Susceptibility modelling of seismically induced effects (landslides and rock falls) integrated to rapid scoring procedures for bridges using GIS tools for the Lowlands of the Saint-Lawrence Valley. Geomatics Nat Hazards Risk. 9(1):589–607.

FEMA. 2003. Multi-hazard loss estimation methodology earthquake model, HAZUS-MH MR3 Technical Manual. Department of Homeland Security, Emergency Preparedness and Response.

Florian D. 2014. Emme 4 Overview: New features, demonstrations and upgrade details, INRO, Montreal, Quebec.

Goda K, Hong H-P. 2008. Spatial correlation of peak ground motions and response spectra. Bull Seismol Soc Am. 98(1):354–365.

Gutenberg B, Richter CF. 1944. Frequency of earthquakes in California. Bull Seismol Soc Am. 34(4):185–188.

Islam MA, Paull DJ, Griffin AL, Murshed S. 2021. Spatio-temporal assessment of social resilience to tropical cyclones in coastal Bangladesh. J Geomatics Nat Hazards Risk. 12(1): 279–309.

Joyner WB, Boore DM. 1993. Methods for regression analysis of strong-motion data. Bull Seismol Soc Am. 83(2):469–487.

Kim Y-S, Spencer Jr BF, Elnashai AS. 2008. Seismic loss assessment and mitigation for critical urban infrastructure systems. Urbana, IL: Newmark Structural Engineering Laboratory. University of Illinois at Urbana; p. 1940–9826.

Korea S. 2016. Results of the 2015 population and housing census (population, household and housing). Population census (National Report).

Lee Y-J, Song J, Gardoni P, Lim H-W. 2011. Post-hazard flow capacity of bridge transportation network considering structural deterioration of bridges. Struct Infrastruct Eng. 7(7-8): 509–521.

Liu Y, Li Z, Wei B, Li X, Fu B. 2019. Seismic vulnerability assessment at urban scale using data mining and GIScience technology: application to Urumqi (China). Geomatics Nat Hazards Risk. 10(1): 958–985.

Loperte S, Calvello M, Faruolo M, Giocoli A, Alfredo Stabile T, Trippetta S. 2019. The contribution of the scientific research for a less vulnerable and more resilient community: the Val d'Agri (Southern Italy) case. J Geomatics Nat Hazards Risk. 10(1):873–897.
Mackie K, Stojadinović B. 2006. Post-earthquake functionality of highway overpass bridges. Earthq Eng Struct Dyn. 35(1):77–93.
Masoomi H, Burton H, Tomar A, Mosleh A. 2020. Simulation-based assessment of postearthquakefunctionality of buildings with disruptions to cross-dependent utility networks. J Struct Eng. 146(5):04020070.
Mebarki A, Jerez S, Prodhomme G, Reimeringer M. 2016. Natural hazards, vulnerability and structural resilience: tsunamis and industrial tanks. J Geomatics Nat Hazards Risk. 7(sup1): 5–17.
Misra S, Padgett JE, Barbosa AR, Webb BM. 2020. An expert opinion survey on post-hazard restoration of roadways and bridges: Data and key insights. Earthq Spectra. 36(2):983–1004.
Mitoulis SA, Argyroudis SA, Loli M, Imam B. 2021. Restoration models for quantifying flood resilience of bridges. Eng Struct. 238:112180.
Murachi Y, Orikowski MJ, Dong X, Shinozuka M. 2003. Fragility analysis of transportation networks. Smart Structures and Materials 2003: Smart Systems and Nondestructive Evaluation for Civil Infrastructures.
Nuti C, Rasulo A, Vanzi I. 2007. Seismic safety evaluation of electric power supply at urban level. Earthq Eng Struct Dyn. 36(2):245–263.
Nuti C, Rasulo A, Vanzi I. 2009. Seismic assessment of utility systems: Application to water, electric power and transportation networks. Safety, Reliability and Risk Analysis. Theory, Methods and Applications. Proc Joint.
Ouyang M, Wang Z. 2015. Resilience assessment of interdependent infrastructure systems: With a focus on joint restoration modeling and analysis. Reliab Eng Syst Saf. 141:74–82.
Padgett JE, DesRoches R. 2007. Bridge functionality relationships for improved seismic risk assessment of transportation networks. Earthq Spectra. 23(1):115–130.
Parvez IA. 2013. New approaches for seismic hazard studies in the Indian subcontinent. J Geomatics Nat Hazards Risk. 4(4):299–319.
Poljanšek K, Bono F, Gutiérrez E. 2012. Seismic risk assessment of interdependent critical infrastructure systems: The case of European gas and electricity networks. Earthq Eng Struct Dyn. 41(1):61–79.
Porter KA. 2004. A survey of bridge practitioners to relate damage to closure. Pasadena (CA): California Institute of Technology.
Rokneddin K, Ghosh J, Dueñas-Osorio L, Padgett JE. 2013. Bridge retrofit prioritisation for ageing transportation networks subject to seismic hazards. Struct Infrastruct Eng. 9(10): 1050–1066.
Sanchez-Silva M, Daniels M, Lleras G, Patino D. 2005. A transport network reliability model for the efficient assignment of resources. Transport Res B-Meth. 39(1):47–63.
Shafieezadeh A, Burden LI. 2014. Scenario-based resilience assessment framework for critical infrastructure systems: case study for seismic resilience of seaports. Reliab Eng Syst Saf. 132:207–219.
Sharma TA, Gardoni P. 2020. Regional resilience analysis: A multiscale approach to optimize the resilience of interdependent infrastructure. Computer-Aided Civil Infrastructure Engineering.
Sharma S, Mathew TV. 2011. Multiobjective network design for emission and travel-time trade-off for a sustainable large urban transportation network. Environ Plann B Plann Des. 38(3):520–538.
Shinozuka M, Murachi Y, Dong X, Zhou Y, Orlikowski MJ. 2003. Effect of seismic retrofit of bridges on transportation networks. Earthq Eng Eng Vib. 2(2):169–179.
Tak H-Y, Suh W, Lee Y-J. 2019. System-level seismic risk assessment of bridge transportation networks employing probabilistic seismic hazard analysis. Math Prob Eng. 2019:1–17.

Wagener T, Goda K, Erdik M, Daniell J, Wenzel F. 2016. A spatial correlation model of peak ground acceleration and response spectra based on data of the Istanbul earthquake rapid response and early warning system. Soil Dyn Earthq Eng. 85:166–178.

Yoon S, Kim J, Kim M, Tak H-Y, Lee Y-J. 2020. Accelerated system-level seismic risk assessment of bridge transportation networks through artificial neural network-based surrogate model. Appl Sci. 10(18):6476.

Yoon S, Lee DH, Jung H-J. 2019. Seismic fragility analysis of a buried pipeline structure considering uncertainty of soil parameters. Int J Press Vessel Pip. 175:103932.

Yoon S, Lee Y-J, Jung H-J. 2018. A comprehensive framework for seismic risk assessment of urban water transmission networks. Int J Disaster Risk Reduct. 31:983–994.

Yoon S, Lee Y-J, Jung H-J. 2020. A comprehensive approach to flow-based seismic risk analysis of water transmission network. Struct Eng Mech. 73(3):339–351.

Zhang W, Wang N, Nicholson C. 2017. Resilience-based post-disaster recovery strategies for road-bridge networks. Struct Infrastruct Eng. 13(11):1404–1413.